Obrabotka metallov (tekhnologiya, oborudovanie, instrumenty) = Metal Working and Material Science. 2022 vol. 24 no. 2 pp. 6–24
ISSN: 1994-6309 (print) / 2541-819X (online)
DOI: 10.17212/1994-6309-2022-24.2-6-24

NSTU NETI

Obrabotka metallov -
Metal Working and Material Science

Journal homepage: http://journals.nstu.ru/obrabotka_metallov

Machining technology, digital modelling and shape control device for large parts

Sergey Timofeev [1, a], *Anna Grinek* [2, b, *], *Andrej Hurtasenko* [3, d], *Igor Boychuk* [2, c]

[1] Limited Liability Company «Promagro», 370a Rzhevskoe shosse, Shebekino, 309290, Russian Federation
[2] Admiral Ushakov State Maritime University, 93 Lenin's avenue, Novorossiysk, 353918, Russian Federation
[3] Belgorod State Technological University named after V.G. Shukhov, 46 Kostyukova st., Belgorod, 308012, Russian Federation

[a] https://orcid.org/0000-0002-6740-5163, timofeevsp@inbox.ru, [b] https://orcid.org/0000-0001-7953-3501, grinyokann@gmail.com,
[c] https://orcid.org/0000-0002-2614-5457, hurtintbel@mail.ru, [d] https://orcid.org/0000-0002-1996-2184, boychuk@ieee.org

ARTICLE INFO

Article history:
Received: 16 February 2022
Revised: 14 March 2022
Accepted: 23 March 2022
Available online: 15 June 2022

Keywords:
Digital simulation
Large parts
Riding ring
Shape measurement
Mechanical restoration

ABSTRACT

Introduction. The development of a method for controlling the accuracy parameters of large axisymmetric bodies is an urgent task that is being solved by specialists from various industries. Application for adjustment and correction of machining based on the measurement of surface shape parameters directly during machining is shown. **Purpose of work** is to improve mobile processing technologies using special measuring devices and processing module. For this, the problems of development and analysis of mathematical models that describe the process of basing and machining of a riding ring as a cylindrical object with a non-stationary axis of rotation is solved. A study of the methodology is carried out, control schemes are designed, and equipment for processing mobile devices is developed. **The methods of research** are the analysis of the developed mathematical models, taking into account the assignment of effective technological modes. Three-dimensional and simulation modeling of processing, hardware-software implementation of proposed solutions, and statistical processing of measurement results are carried out. **Results and discussion.** The algorithm and methodology are tested with a three-dimensional simulation model. The presented methodology for measuring and calculating the allowance for mechanical restoration can significantly reduce machining time compared to active form control and compared to the traditional method of assigning an allowance for machining. The measurement and adjustment of the allowance based on the measurement data is not carried out after each measurement, but only in the case of transition to finishing transitions or for accuracy control. It is determined that by providing a single technological base for each individual technological transition within the framework of the mobile technology of machining of the rolling surface of the riding rings of technological drums, the accuracy and speed of processing increase. An original design of the device for monitoring parameters is developed; an experimental assembly and a laboratory model of the riding ring are made.

For citation: Timofeev S.P., Grinek A.V., Hurtasenko A.V., Boychuk I.P. Machining technology, digital modelling and shape control device for large parts. *Obrabotka metallov (tekhnologiya, oborudovanie, instrumenty) = Metal Working and Material Science*, 2022, vol. 24, no. 2, pp. 6–24. DOI: 10.17212/1994-6309-2022-24.2-6-24. (In Russian).

Introduction

Large tubular, drum-type rotating units ranging in length from several tens to several hundred meters are used in a number of industries [1, 2]. Its characteristic feature is a unified operating principal, which includes continuous movement of large masses of material with its parallel treatment: heating, grinding, washing [3, 4]. The development of a method to control the accuracy parameters of large rotary bodies is an urgent task being solved by specialists from various industries [5]. The shape defects are associated not only with large size and weight, but also with the location conditions of the units, under which the position of the rotation axis is not constant. This factor also determines the specifics of the work to ensure the accuracy

*** Corresponding author**
Grinek Anna V., Ph.D. (Engineering), Associate Professor
Admiral Ushakov State Maritime University,
93 Lenin's avenue,
353918, Novorossiysk, Russian Federation
Tel.: +7-960-637-38-82, **e-mail**: grinyokann@gmail.com

of the shape of these surfaces by machining during the technological rotation of the unit [6, 7]. Hence, it is critical to develop a technology ensuring the shape accuracy of the rolling surface of riding rings, for which it is possible to calculate the modes and predict the result of processing. It is important for this technology to apply active methods to control the processing based on the measurement of surface accuracy parameters directly during processing. At the same time, the most relevant issues include modeling and calculation of processing modes based on data obtained after measurement [8]. The introduction of the mechanical processing technology with regard to rollers and riding rings of cement kilns and elements of any large structures requires the development and manufacture of special equipment, namely a measuring device and a processing module [9].

The most complete information on a complex technical system obtained on the basis of mathematical modeling and measurement serves the basis for the design of automated and regulated technological processes [10–12].

Solutions in the field of measuring cylindrical parts and calculating the shape error [13-16] in conditions of basing uncertainty, complex operating conditions are based on statistical and deterministic mathematical models describing cylindrical bodies in statics and dynamics. There are mathematical models describing the behavior of cement kiln elements (riding rings, support rollers) and similar units and mechanisms based on various approaches and assumptions [17–19].

There are non-contact measurement systems [20–22] that improve the accuracy of measurements under conditions of vibration and dustiness of cement production, using laser research methods.

Besides, there is a need to develop the appropriate software for these devices. It is obvious that this requires a lot of time and considerable financial costs. Therefore, for the initial analysis of the effectiveness and applicability of the proposed technology, it should be tested using virtual modeling or a digital twin of the riding ring machining process.

The purpose of this work is to improve mobile processing technologies using special measuring devices and processing modules. This will significantly increase the interrepair cycle and reduce the time of mechanical processing of large parts – rotary bodies.

The objectives of the study are to develop and analyze the mathematical models describing the basing and machining of a riding ring as a cylindrical object with a non-stationary rotation axis, to study the proposed methodology, to develop the control schemes and to implement the equipment for mobile machining.

Materials and methods

A full cycle of works was implemented during the study, which utilized the original control method: from determining the shape accuracy parameters to processing simulation along the calculated scheme.

A riding ring is a large cylindrical body with a non-stationary rotation axis. During operation it is based on support rollers, while the unit itself does not have the rotation axis. Typically, the rollers are mounted at an angle of 60° relative to the kiln axis. Depending on the length and weight of such a technological drum, the number of supports may vary from 2 to 8–10 pieces.

The location scheme does not change during repair machining or shape control (without the unit removal), while the processing module with the tool is based on the processed surface, and a centerless processing scheme is implemented. According to one of the existing technologies, the machining of support elements of rotating cement kilns is assigned after detecting the error in the shape of these parts exceeding the specified value.

The shape parameters of the rolling surface of operating kilns riding rings were taken for the virtual model. This allowed a comparative analysis of the machining techniques used. The rolling surface directly adopted for the model (Fig. 1) has a nominal diameter of 6.1 m, a width of 1 m, with a total radial runout value of about 12 mm, and a barrel-shaped profile of the longitudinal section. The virtual model of the riding ring and devices was performed in the *Siemens NX* computer-aided design system.

The calculation of the machining allowance requires data on the accuracy parameters of the shape of the entire machined surface. The following measurement technique with three-dimensional digital

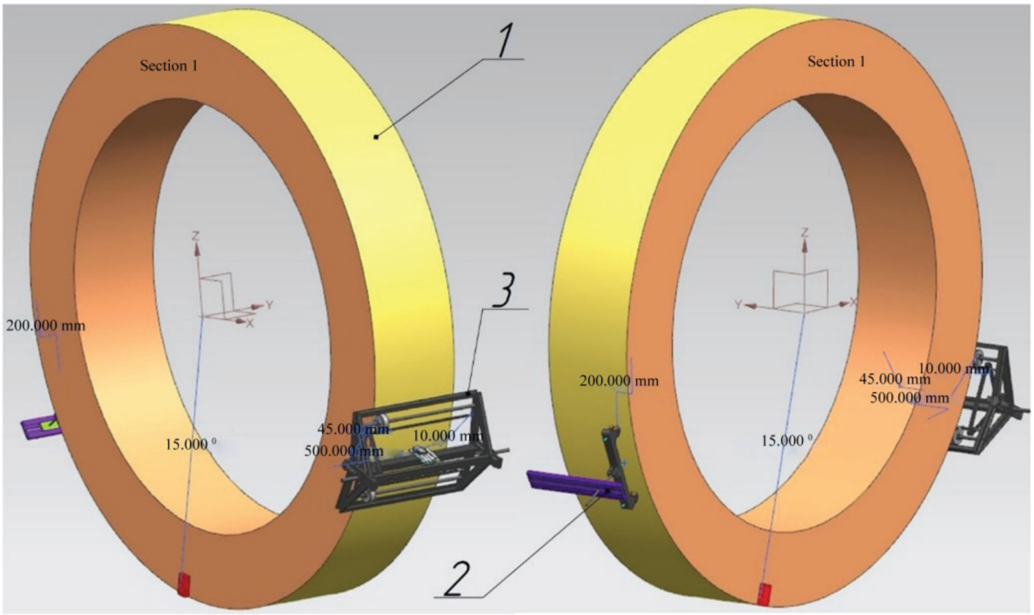

Fig. 1. Virtual model of the riding ring and the virtual models of the measuring device and the processing module installed for processing:
1 – model of the riding ring; *2* – measuring device; *3* – processing module

reconstruction and the implemented measuring device ensure the accuracy of the shape of the technological drum riding rings directly during the technological rotation of the units.

When developing the machining route, the possibility of correcting the accuracy of the surface shape to specified values according to industry standards was investigated, i.e. the deviation of the real profile of the entire surface from the cylinder inscribed in it, $\Delta_{TFZ}^{specified} = 3.05$ mm, using a belt-abrasive method and minimizing the machining allowance (removing the allowance to the dimensions of the inscribed cylinder).

Mathematical models for machining technology and machining simulation

Calculation of the motion trajectory of an independent support copying device (hereinafter referred to as ISCD)

The algorithm for the calculation of the *ISCD* position during its movement along the contour of the base section looks as follows (Fig. 2):

– the axis of the first support roller of the *ISCD* (point P_{ro1}) is aligned with n_{EK} point of the previously obtained equidistant;

– the position of the second support roller of the *ISCD* (point P_{ro2}) is calculated at the equidistance;

– the rotation angle of the local coordinate system of the *ISCD* LCS_{ISCD} relative to $BCS^{general}$ is calculated;

– the equation of the straight line passing through the point of the tip of the cutting tool parallel to the plane of its movement is determined;

– the algorithm is repeated for all equidistant points.

To find the rotation angle of the *ISCD* local coordinate system (LCS_{ISCD}, Fig. 2) there is a need to determine the position of point P_{ro2} for each position in $BCS^{general}$.

Formulas for calculating the rotation angle of LCS_{ISCD} relative to $BCS^{general}$ (1–6) for the *m*-position of the *ISCD* with known coordinates of points P_{ro1} and P_{ro2}:

$$\varphi_m = \operatorname{arctg}\left(\frac{y_{Ppo2\_m} - y_{Ppo1\_m}}{x_{Ppo2\_m} - x_{Ppo1\_m}}\right), \quad \text{at} \quad x_{Ppo2\_m} - x_{Ppo1\_m} > 0 \tag{1}$$

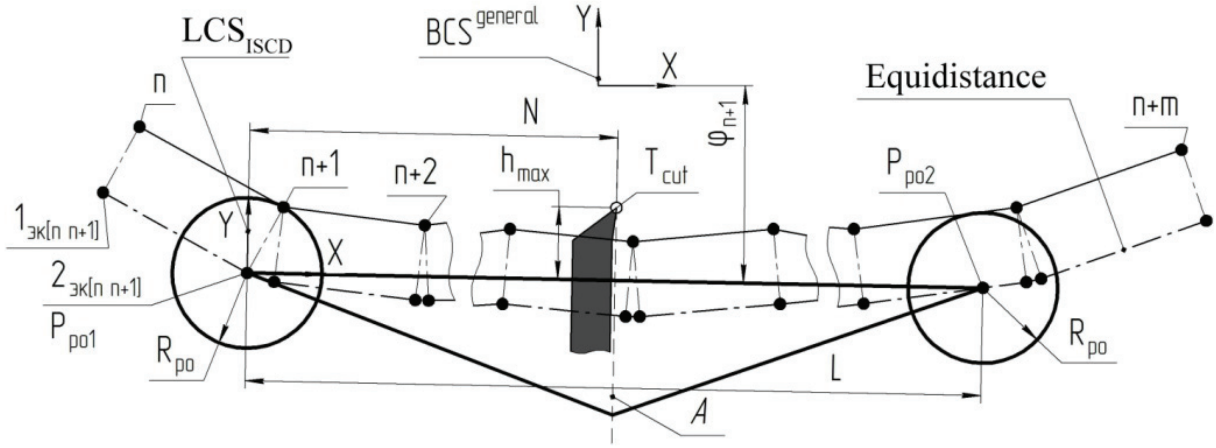

Fig. 2. Schematic diagram of the calculation of the processing module position (A – line corresponding to the axis of movement of the cutting tool edge)

$$\varphi_m = 0 \text{, at } x_{Ppo2\_m} - x_{Ppo1\_m} > 0 \quad \text{and} \quad y_{Ppo2\_m} - y_{Ppo1\_m} = 0 \tag{2}$$

$$\varphi_m = \operatorname{arctg}\left(\frac{y_{Ppo2\_m} - y_{Ppo1\_m}}{x_{Ppo2\_m} - x_{Ppo1\_m}}\right) + \pi, \quad \text{at} \quad x_{Ppo2\_m} - x_{Ppo1\_m} < 0 \tag{3}$$

$$\varphi_m = \pi, \quad \text{at} \quad x_{Ppo2\_m} - x_{Ppo1\_m} < 0 \quad \text{and} \quad y_{Ppo2\_m} - y_{Ppo1\_m} = 0 \tag{4}$$

$$\varphi_m = \frac{\pi}{2}, \quad \text{at} \quad x_{Ppo2\_m} - x_{Ppo1\_m} = 0 \quad \text{and} \quad y_{Ppo2\_m} - y_{Ppo1\_m} > 0 \tag{5}$$

$$\varphi_m = -\frac{\pi}{2}, \quad \text{at} \quad x_{Ppo2\_m} - x_{Ppo1\_m} = \quad \text{and} \quad y_{Ppo2\_m} - y_{Ppo1\_m} < 0, \tag{6}$$

where x_{Ppo1_m} and y_{Ppo1_m} – coordinates of point P_{ro1} in $BCS^{general}$ for *m*-position of the *ISCD*; x_{Ppo2_m} and y_{Ppo2_m} – coordinates of point P_{ro2} in $BCS^{general}$ for *m*-position of the *ISCD*.

Under known coordinates of the axis point of the support roller P_{ro1}, the structural parameters of the *ISCD* and φ_m angle corresponding to the rotation of LCS_{ISCD} relative to $BCS^{general}$, the geometric coordinates of the extreme point of the cutting part of the tool P_{cut} (hereinafter referred to as the cutting point) in $BCS^{general}$ are found according to the formula (7):

$$\begin{pmatrix} x_{Pcut\_m} \\ y_{Pcut\_m} \end{pmatrix} = \begin{pmatrix} x_{Ppo1\_m} \\ y_{Ppo1\_m} \end{pmatrix} + \begin{pmatrix} \cos(\varphi_m) - \sin(\varphi_m) \\ \sin(\varphi_m)\cos(\varphi_m) \end{pmatrix} \begin{pmatrix} N \\ h_{\max} \end{pmatrix}, \tag{7}$$

where x_{Pcut_m} and y_{Pcut_m} – coordinates of the P_{cut} point in $BCS^{general}$ for *m*-position of the *ISCD*.

Then the equation of the straight line passing through the known point P_{cut} along the axis of movement of the cutting tool in the current position of the *ISCD* (line A, Fig. 2) is calculated according to the formula (8):

$$y = k \cdot (x - x_{Pcut\_m}) + y_{Pcut\_m}, \tag{8}$$

where *k* is the coefficient of the inclination angle of the straight line, determined by formula 9:

$$k = \operatorname{tg}\left(\varphi_m + \frac{\pi}{2}\right). \tag{9}$$

For the case where $\varphi_m + \frac{\pi}{2} = \frac{\pi}{2}$, the equation of straight line corresponds to formula (10):

$$x = x_{Pcut\_m}. \quad (10)$$

Calculation of the ISCD motion path

Correcting the accuracy of surface shapes, while ensuring the conditions for removing the maximum allowance and the absence of cutting the surface to an inscribed circular cylinder at each transition, is carried out by calculating the limiting value of the cutting tool overhang per transition $h^I_{\text{p\_max}}$ (where *I* is the transition sequence number). The value $h^I_{\text{p\_max}}$ is determined based on the calculation of the trajectory of the *ISCD* motion trajectory along the contour of the base section of the surface and data on the parameters of the inscribed cylinder (Fig. 3).

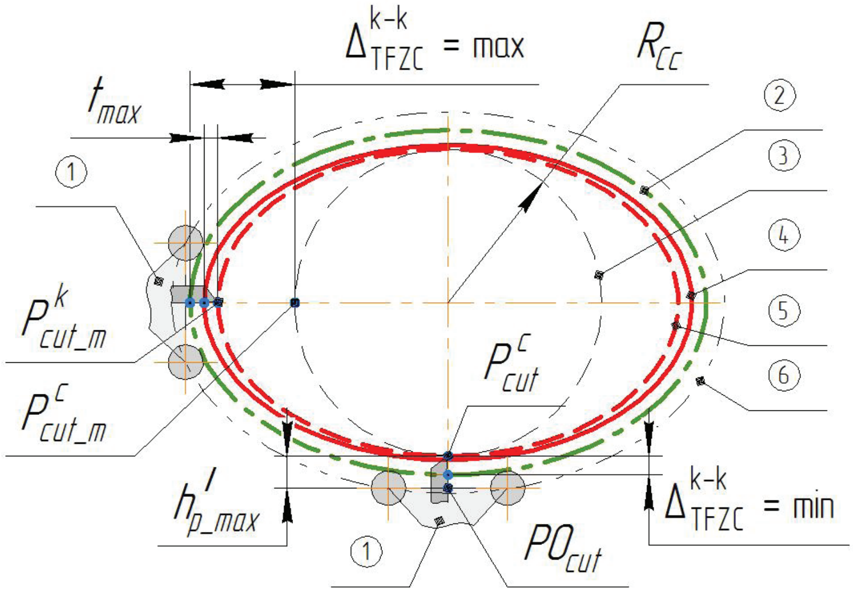

Fig. 3. Schematic diagram for the calculation $h^I_{p\_\max}$ of the transition:

1 – processing module; *2* – contour of the base section; *3* – contour of the inscribed circular cylinder; *4* – contour of the surface before machining at the transition; *5* – contour surface after machining for a wide transition; *6* – equidistant to the contour of the technological section; *k-k* – surface area suitable for this base

The calculation algorithm for $h^I_{p\_\max}$ is the following sequence:

1. The point of intersection of the straight line corresponding to the axis of movement of the cutting tool in the current position of the *ISCD* (Equation (8)), with the contour of the section of the inscribed circular cylinder $P^C_{cut\_m}$ is calculated.

2. The distance from the point $P^C_{cut\_m}$ to the zero point $P0_{cut\_m}$ of the *ISCD* is calculated (the point at which the cutting tool overhang is taken as $h^I_p = 0$). The calculation is made according to formulas (11) and (12):

$$h^I_{p\_m} = \sqrt{(x_{Pcut\_m} - x_{P0\_m})^2 + (y_{Pcut\_m} - y_{P0\_m})^2}, \quad (11)$$

where x_{P0cut_m} and y_{P0cut_m} are the coordinates of the point $P0_{cut\_m}$ in $BCS^{general}$ for the m-position of the *ISCD*, determined by the formula:

$$\begin{pmatrix} x_{P0cut\_m} \\ y_{P0cut\_m} \end{pmatrix} = \begin{pmatrix} x_{Ppol\_m} \\ y_{Ppol\_m} \end{pmatrix} + \begin{pmatrix} \cos(\varphi_m) - \sin(\varphi_m) \\ \sin(\varphi_m)\cos(\varphi_m) \end{pmatrix} \begin{pmatrix} N \\ 0 \end{pmatrix}. \quad (12)$$

3. From the obtained distances the minimum value is selected and is set as $h^I_{p\_\max}$.

4. Points P^k_{cut} are calculated for all positions of the *ISCD* with a cutting tool overhang equal to $h^I_{p\_\max}$. Based on the obtained points P^k_{cut}, a *B*-spline is constructed, which determines the maximum achievable shape of the surface section contour after machining at a given transition (line 5, Fig. 4). The calculated value $h^I_{p\_\max}$ determines the maximum allowance to be removed at the *I*-transition, which provides machining of the surface to the dimensions of an inscribed circular cylinder (without gouging).

Calculation of the maximum cutting depth

From the adopted processing scheme and strategy for setting the working strokes it follows that the actual cutting depth is a variable and depends on the *ISCD* motion trajectory along the base surface section, as well as on the distortion of the surface shape in the section being processed. Thus, it is possible to exceed the maximum permissible cutting depth $t^{per}_{\max}$ (*per.* – permissible), at which the cutting tool and/or the processing module will fail. In order to prevent this failure it is necessary to calculate the maximum achieved cutting depth $t^k_{\max}$ (Fig. 4) in each k^{th} cross section of the processing area for the current parameters of the limit value of the cutting tool extension $h^I_{p\_\max}$ to the technological transition.

The value $t^k_{\max}$ in the k^{th} section on the basis of the previously given model of the forming process is calculated according to the following algorithm.

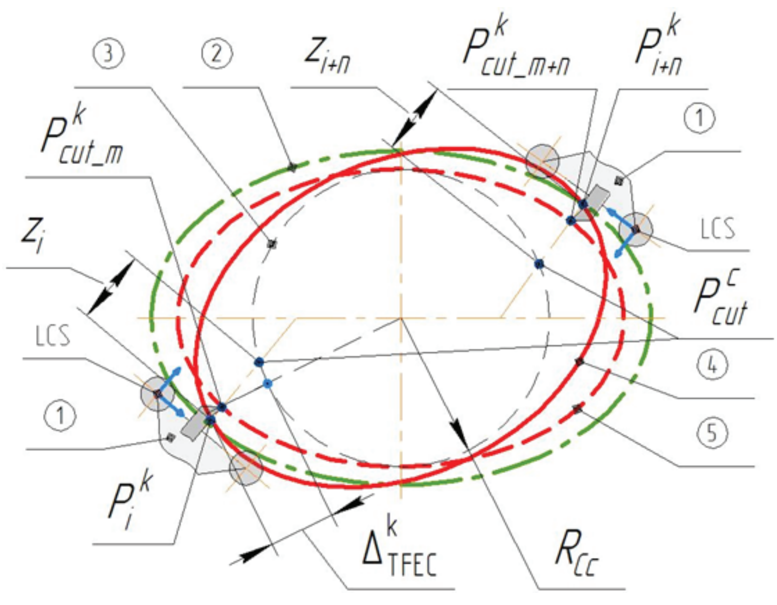

Fig. 4. Schematic diagram of calculating the depth of cut in the k^{th} section

1 – processing module; *2* – base section contour; *3* – inscribed circular cylinder contour; *4* – surface contour before machining at the current transition; *5* – calculated surface contour after machining for the current transition; z_i – is the calculated maximum machining allowance for the current transition and the position of the *NOUK*

Calculation of the tool cut-in points for each ISCD position

The coordinates of point P_i^k (Fig. 4) corresponding to the intersection of the straight line, along which the cutting tool is moved (equation (8)) with the contour of the cross-section of surface 4 (Fig. 4), are calculated prior to processing for each of the known *ISCD* positions obtained during the $h_{p\_\max}^I$ calculation.

Each point $P_{cut\_m}^k$ should correspond to only one point P_i^k, however, in the general case, the solution has two points of intersection of the straight line (equation (8)) and the contour of the processed section of surface 4 (Fig. 4). Therefore, for further calculations, a point is taken for which the modulus of distance from the point P_{cut}^k is the smallest.

Results and discussion

Determination of shape accuracy parameters of a virtual riding ring model

To determine the accuracy parameters of the shape of the rolling surface of the virtual riding ring model, its virtual reconstruction was carried out based on the measurement of 6 cross sections. Each section was 200 mm apart from the adjacent one, with the extreme sections coinciding with the edges of the model.

A parameterized virtual model of the measuring device (Fig. 1) corresponding to the original basic patented scheme of the measuring device, as well as a software module (Fig. 5) implementing an algorithm for calculating the accuracy parameters of the cross-section shape were used for experimental measurements and to check the operability of solutions.

Fig. 6 shows the calculated distribution of Δ_{TFEC}^k for sections with the maximum and minimum value of the shape error.

The combined diagram of section contours and the inscribed cylinder are shown in Fig. 7. The obtained calculation data on the accuracy parameters of the rolling surface shape are used for further analysis and development of the machining route.

Construction of a machining route

According to the proposed technology, the processed surface was initially analyzed according to the data on its geometric parameters of shape accuracy obtained at the measurement stage.

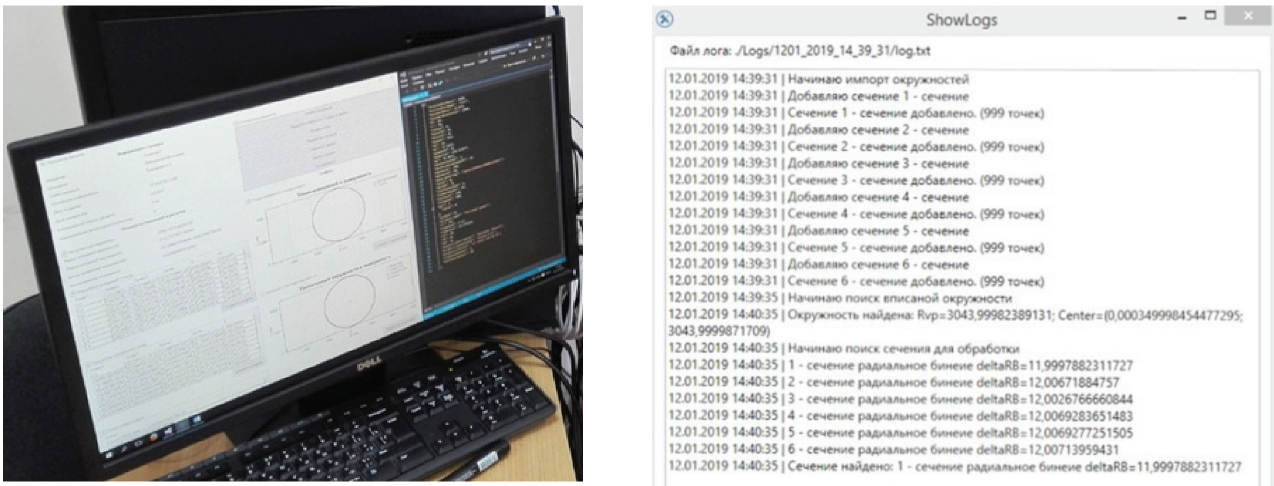

a *b*

Fig. 5. Software implementation of the shape calculation algorithm:

a – program user interface; *b* – log window when calculating surface shape parameters

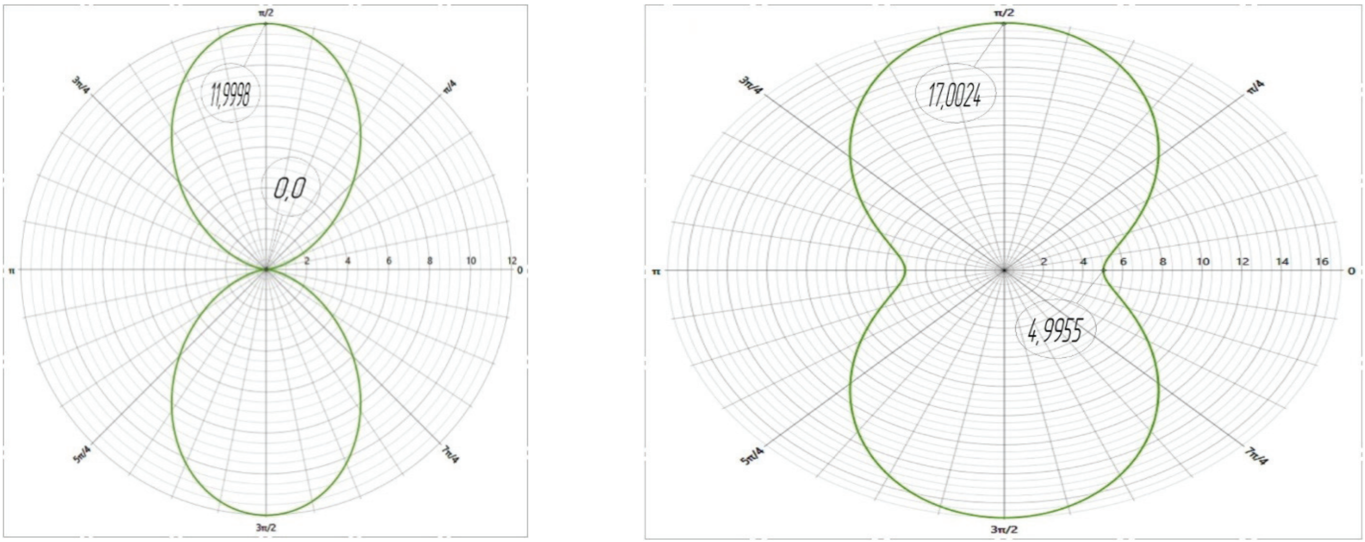

a *b*

Fig. 6. Round diagrams of the shape deviation distribution of the verification sections:
a – section No.1; *b* – section No.4

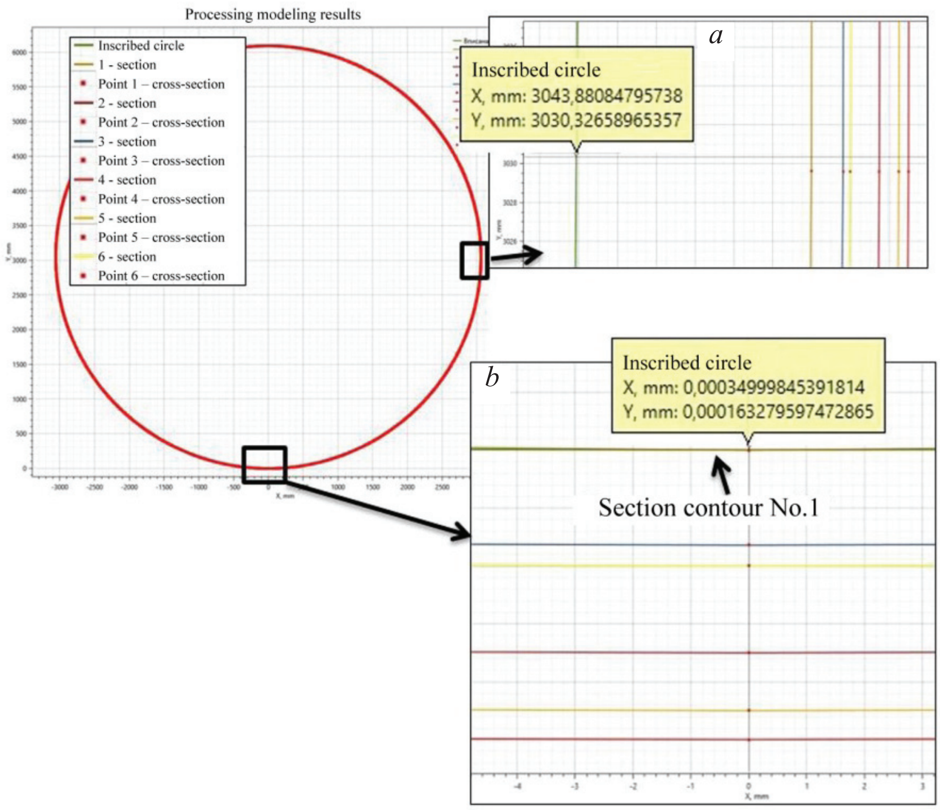

Fig. 7. Combined diagram of the contours of the sections and the inscribed cylinder:
a – plot of the graph in the region of the minimum error in the shape of the surface;
b – plot of the graph in the region of the maximum error in the shape of the surface

It follows from the data analysis that section No.1 has the smallest value of the parameter Δ^1_{ECR} , as well as Δ^1_{TFEC}. At the same time, section No.2 has one of the smallest shape errors. Thus, according to the proposed processing scheme, a surface area from section No.1 to section No.2 is taken as a possible surface area for the location of the processing module. Besides, in view of the accepted width of the support rollers of the processing module, a section with a width of 100 mm from section No.1 is taken for the main technological base at the first transition. The section is hereinafter designated as *M*-1.

In the process of the 1st technological transition, the processing module is based on an unprocessed surface, and since the profile of the longitudinal section in this area has non-rectilinear generatrices, the calculated trajectory of the *ISCD* will differ from the actual one. Therefore, the following rules are adopted for the machining route:

The calculation of the trajectory of the movement of the *ISCD* should be be carried out along the cross section of the main technological base with a minimum value of Δ_{TFEC}^{k}. Besides, $h_{p\_\max}^{I}$ is also calculated for this section.

When calculating the values of $h_{pG}^{I,k-k}$, in order to exclude the possibility of exceeding the maximum permissible value $t_{\max}^{per}$, in the case of severe wear of the rolling surface of the riding ring, a corresponding reduction $t_{\max}^{per}$ is necessary.

After performing the 1st transition, it is necessary to perform the operation of determining the geometric parameters of the accuracy of the shape of the machined surface areas and adjust the calculation of the machining route according to the data obtained.

After performing the 1st transition it is necessary to determine the geometric parameters of the shape accuracy of processed surface sections and correct the calculation of the machining route based on the obtained data.

In order to reduce the main processing time, it is rational to machine two small and adjacent surface areas (sections *M*-1 and *M*-2) until the required shape accuracy parameters are obtained on one of them. After obtaining a surface area with the required shape error, it is taken as the main technological base for processing the entire remaining surface. Thus, at the 1st transition, the calculation and simulation of the processing of a surface area 100 mm wide adjacent to the main technological base – *M*-2 – was performed (Fig. 8).

According to the calculation of the parameters of the machining route technological modes in the developed software, the maximum cutting depth of the $t_{k\_\max}$ machined section *M*-1 for the 1st transition was

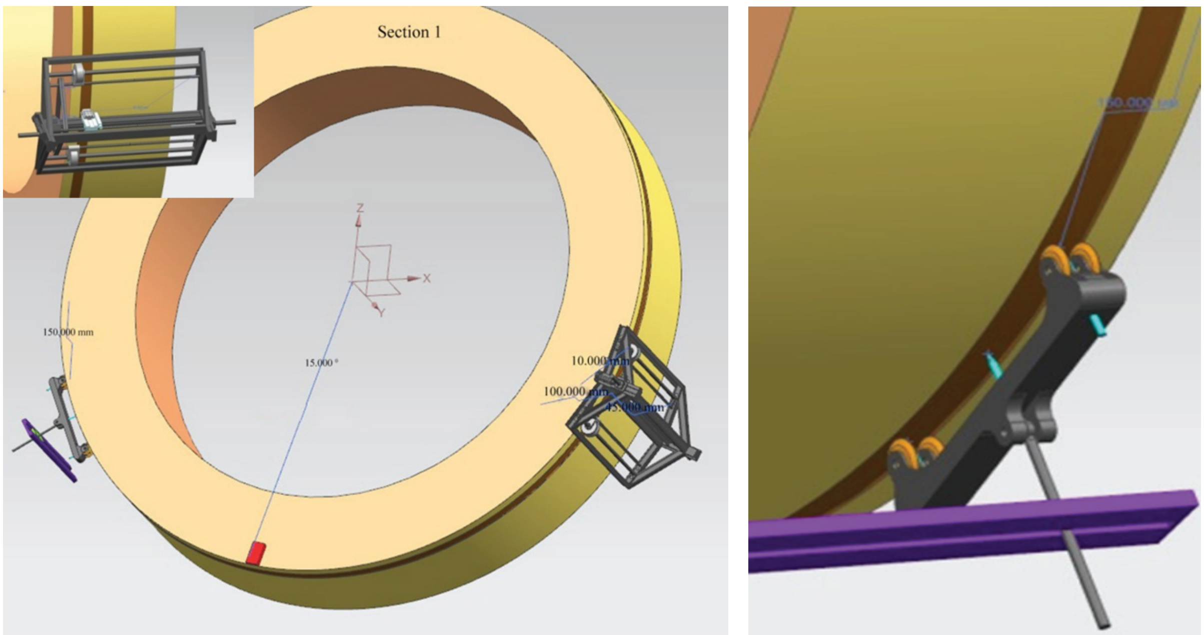

Fig. 8. Machining simulation result after first transition

2.247 mm at $h^{I}_{p\_\max} = 56.21$ mm. In this case, the value Δ^{2}_{ECR} of the processed area should decrease by 0.48 mm and amount to $\Delta^{2}_{ECR} = 11.527$ mm.

According to the results of virtual simulation of the machining process in *CAD NX* for the value of $h^{I}_{p\_\max}$, followed by the determination of the geometric parameters of shape accuracy, the maximum depth of cut t_{k_max} was 1.957 mm (Fig. 9, *a*). The value Δ^{2}_{ECR} of the processed area decreased by 0.34 mm and amounted to $\Delta^{2}_{ECR} = 11.667$ mm (Fig. 9, *b*). Accordingly, the actual output parameters of the geometric accuracy of the shape of the machined section *M*-1 were slightly worse than the calculated ones. The obtained data was transferred to correct the machining route.

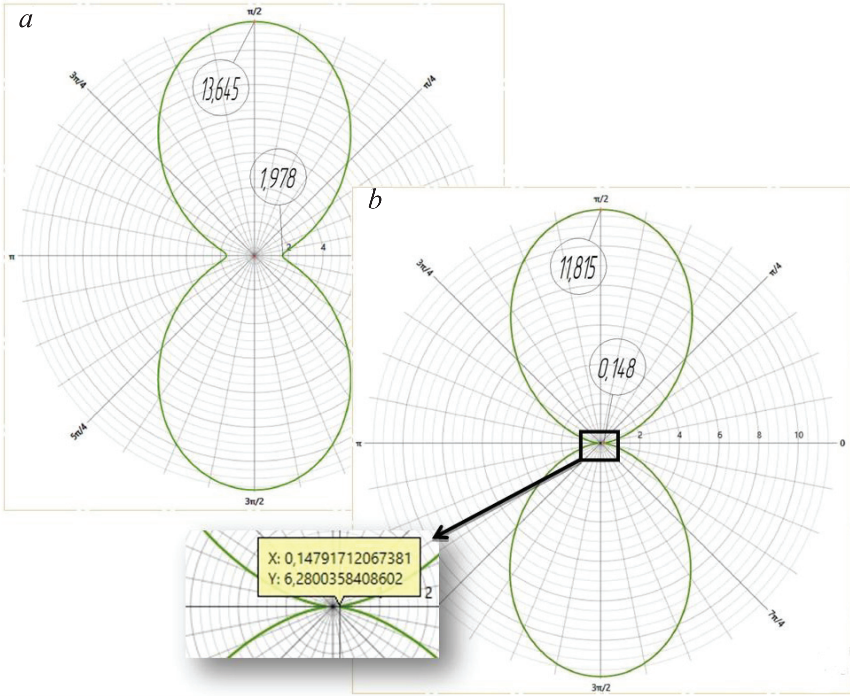

Fig. 9. Round diagram of the shape deviation of the contour of the processed surface area at the 1st transition:
a – before processing; *b* – after processing

The calculation and simulation of processing showed that the proposed processing scheme allows at each individual transition to correct the geometric accuracy of the shape only to the final value. So, for example, at the 2nd transition the maximum value of Δ^{1}_{ECR} achieved for the processed *M*-1 area was 11.365 mm (Fig. 10, *a*). Besides, in case $h^{2}_{p\_\max}$ exceeds the calculated value, a decrease in the radius of the inscribed cylinder R_{Cc} is observed.

The further machining route also assumed the processing of two adjacent surface sections *M*-1 and *M*-2, between sections No.1 and No.2 until the standard value of Δ^{k}_{ECR} was reached. At the same time, before each technological transition, the main technological base was changed to the area processed at the previous transition $\left(\text{with a minimum value of } \Delta^{k}_{ECR}\right)$.

According to the calculations, the standard value of the radial runout is achieved in the *M*-2 are in 51st technological transition (according *to OST 22-170-87* for the weld-in riding ring of a cement kiln with a

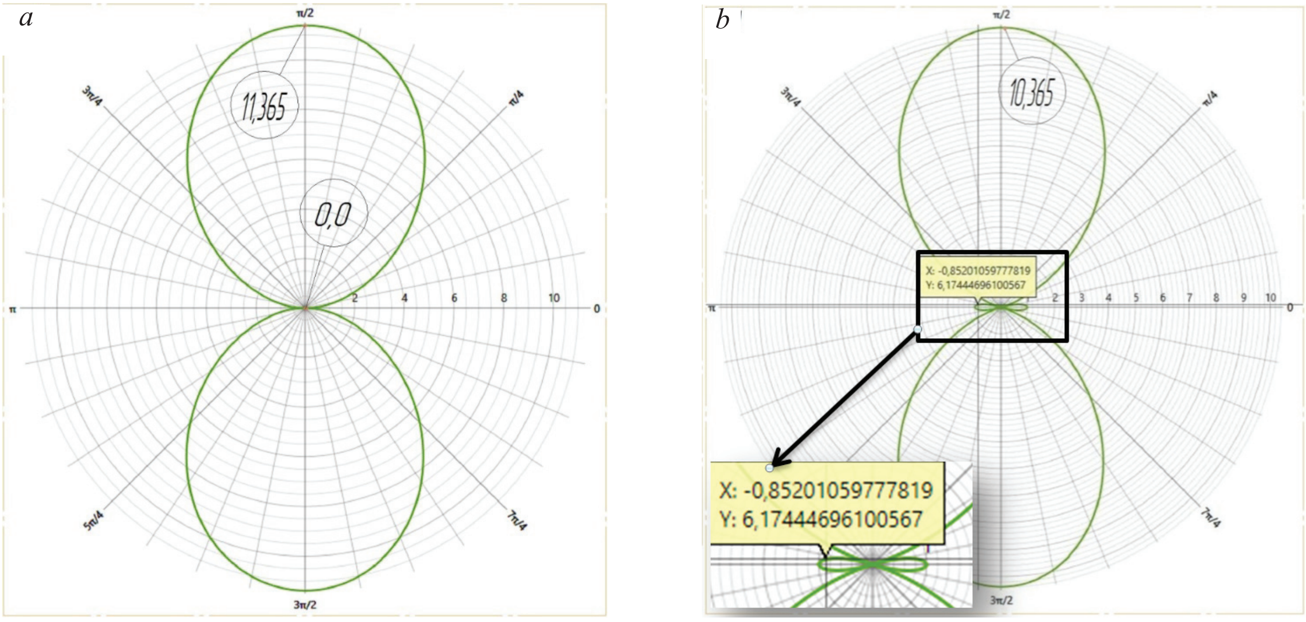

Fig. 10. Round diagram of the shape deviation of the cross-sectional contour of the machined area after the 2nd transition:

$a - h_{p\_\max}^{2} = 56.2$ mm; $b - h_{p\_\max}^{2} = 57.2$ mm

diameter of ø6.1 m, the value is $\Delta_{ECR}^{specified} = 3.04\ \text{mm}\big)$. After performing the 51st transition in section *M*-2, the value $\Delta_{ECR}^{M-2} = 2.998$ mm, and in section *M*-1, the value is $\Delta_{ECR}^{1-M} = 3.082$ mm. Thus, the surface area *M*-2 will be further used for the last technological transition, which involves machining the entire remaining part of the surface. Fig. 11 shows a graph of the change in the Δ_{ECR}^{k} value of the cross sections of the processed surface areas *M-1* and *M*-2 from the 1st to the 51st transition inclusive.

Prior to the last transition, an operation was performed to determine the geometric parameters of the shape accuracy of the *M*-2 surface area, which is taken as the main processing base for the 52nd transition.

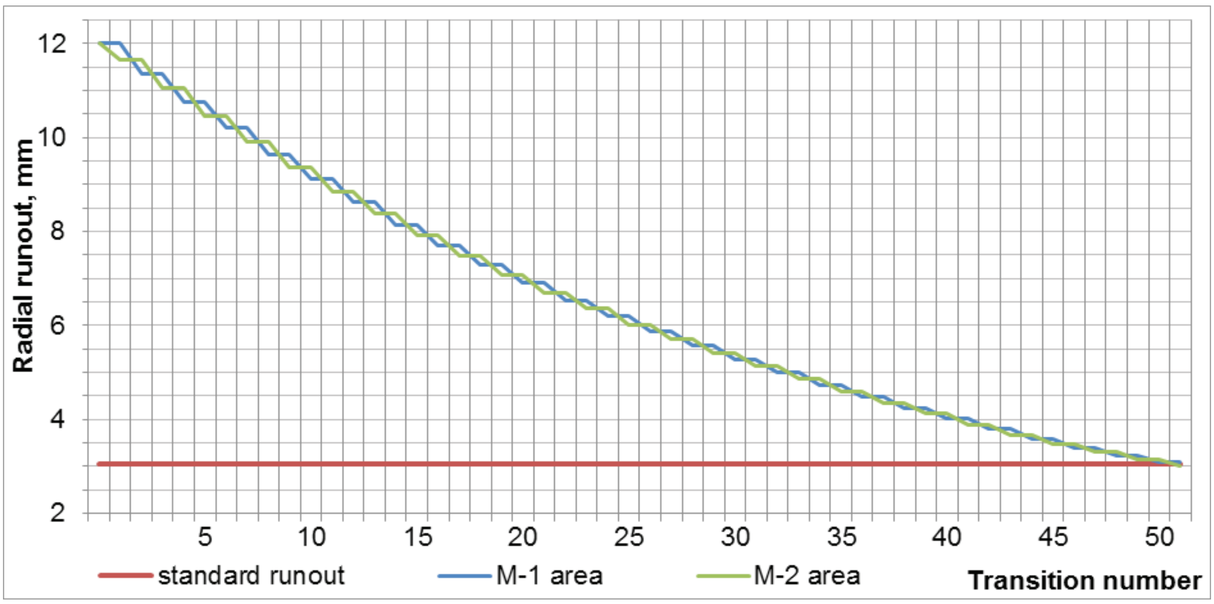

Fig. 11. Graph of the change in the Δ_{ECR}^{k} value of the cross sections of the processed surface areas *M*-1 and *M*-2 from the 1st to the 51st transition inclusive

The need to perform this operation is due to the fact that if the actual value of the shape error in this area is exceeded, the required parameters of geometric accuracy of the rolling surface shape per the calculated number of working strokes during the last transition may fail to be achieved.

The results of the virtual simulation of the machining process in *CAD NX* made it possible to conclude that the actual parameters of the geometric accuracy of the shape of *M*-2 area correspond to the calculated ones. Thus, no correction of the machining route was required.

According to calculations, in order to ensure the specified accuracy of the shape of the entire remaining surface at the 52nd transition it is necessary to produce 14 working strokes characterized by a different amount of cutting tool extension for each surface area. At the same time, the 15th working stroke with the processing depth of 0.07 mm was introduced to ensure the required surface quality (Ra 6.3–12.5 μm).

Fig. 12 shows the computed distribution of the maximum machining allowance for each machined area and working stroke.

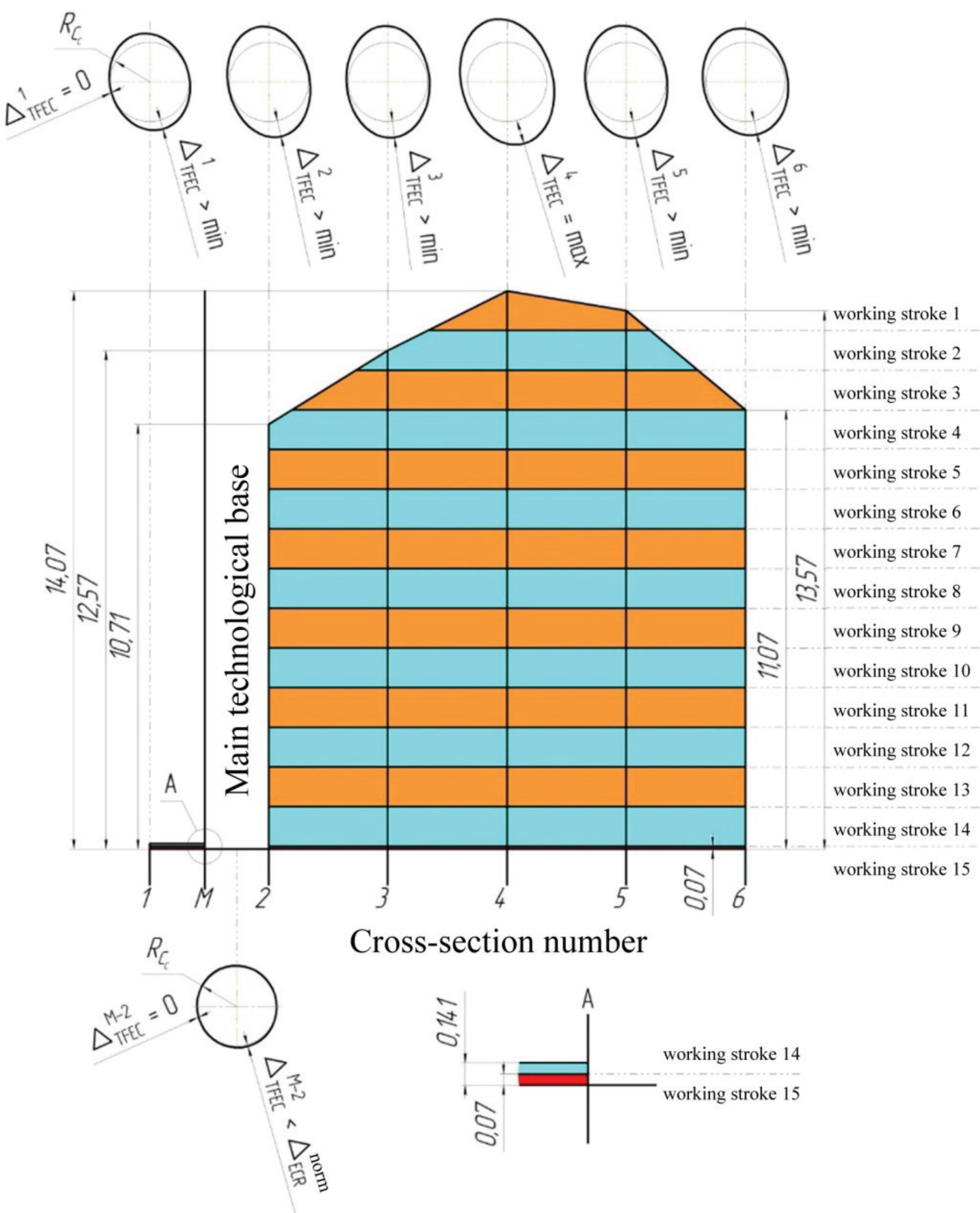

Fig. 12. Distribution of maximum allowances for processing a surface area on a working stroke of the 52nd transition

Simulation and determination of geometric parameters of the accuracy of the rolling surface shape at the 52nd transition using *CAD* confirmed the reliability of the calculated processing modes and the resulting error values.

The main processing time along the specified route taking into account processing until the stop and the riding ring revolution rate of ~ 1 rpm will be:

1st transition:

$$\frac{2 \text{ pass } \times 100 \text{ mm}}{50 \text{ mm/rev} \times 1 \text{ rpm}} + \frac{2 \text{ rev } \times 2 \text{ pass}}{1 \text{ rpm (for cutting extension)}} = 8 \text{ min}; \quad (13)$$

51st transition:

$$\frac{5 \text{ pass } \times 100 \text{ mm}}{50 \text{ mm/rev} \times 1 \text{ rpm}} + \frac{2 \text{ rev } \times 50 \text{ pass}}{1 \text{ rpm}} = 200 \text{ min}; \quad (14)$$

52nd transition:

$$\frac{2 \text{ pass } \times 100 \text{ mm}}{50 \text{ mm/rev} \times 1 \text{ rpm}} + \frac{1 \text{ pass } \times 600 \text{ mm}}{50 \text{ rpm} \times 1 \text{ rpm}} + \frac{14 \text{ pass } \times 800 \text{ mm}}{50 \text{ mm/rev} \times 1 \text{ rpm}} + \frac{2 \text{ rev } \times 15 \text{ pass}}{1 \text{ rpm}} = 200 \text{ min}. \quad (15)$$

The total processing time was 478 minutes or 7.97 hours.

Using a virtual model when assigning a technological allowance for machining

The algorithm for measuring and determining the accuracy parameters of the cross-sectional shape may be implemented in a processing machine module. The enlarged scheme of the proposed technology is divided into two main stages: calculation and simulation of the processing route, machining and preset operations to determine the shape accuracy.

To calculate the technological allowance, an analysis of the machined surface is carried out according to the data on its parameters obtained at the measurement stage.

Then, the current technological base for the next pass is determined based on the calculation results, and the parameters of the processing module are adjusted based on the calculations.

After machining, the geometric parameters of the shape are checked and the process route is adjusted.

The measured surface and the regulatory requirements for the surface are used as the initial data for calculations.

The essential difference of this technology is that processing is carried out up to the parameters of the maximum inscribed circular cylinder, taking into account regulatory requirements, but, if necessary, it can be processed more accurately.

Processing is performed until the required shape accuracy reaches the desired value. Based on the results of the virtual simulation of the machining process in *CAD NX*, the actual parameters of the shape accuracy correspond to the calculated ones. Thus, no adjustment of the machining route was required.

Development and manufacture of a measuring device

To implement the above algorithm for measuring the shape accuracy parameters, an experimental sample of the measuring device [23] was developed; its scheme is shown in Fig. 13 [23].

Fig. 14 and 15 show the implemented design of the experimental surface shape control measuring device based on sensors and electronic components of the domestic manufacturer [24].

The experimental assembly (Fig. 15) consists of a base plate (1) on which one roller support (2) and an experimental model of the measuring device (3) are hinged. The model of the body (4) with its external surface rests on support roller and probes of the surface measuring device. The side surface of the body model rests on adjustable supports of the base plate.

After assembling and connecting the measuring device model to the computer (5), the measuring algorithm was debugged. With this arrangement, the required number of degrees of freedom of the surface

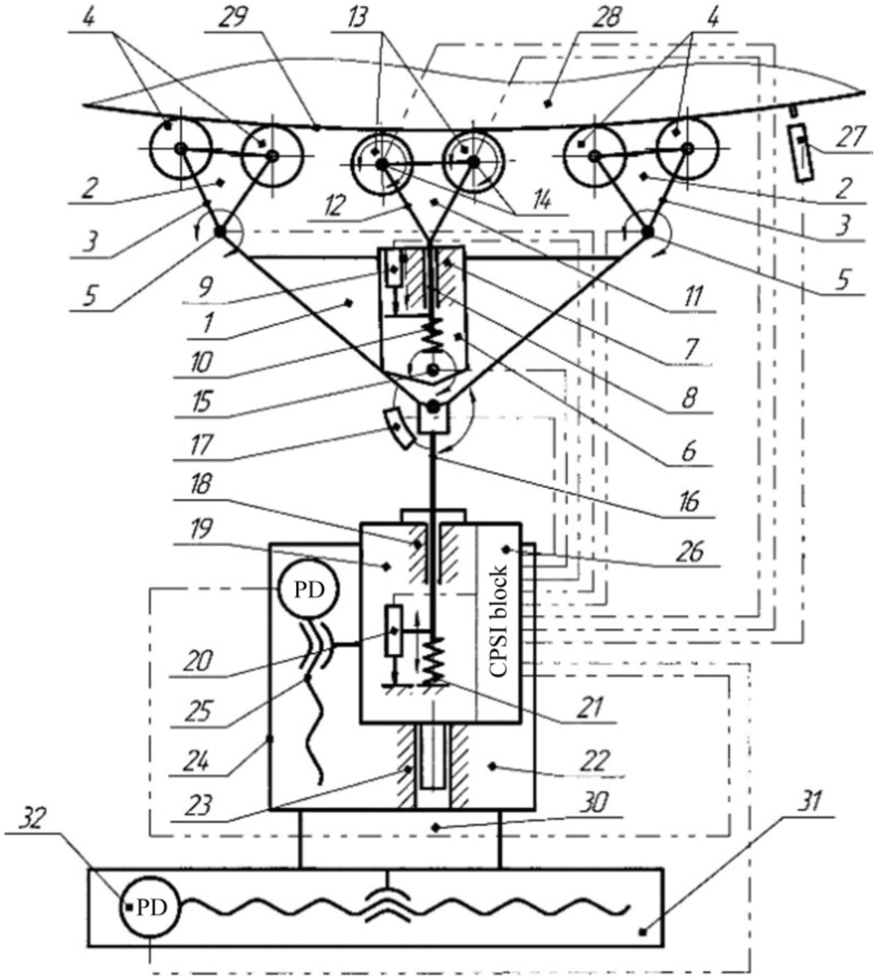

Fig. 13. Device for measuring product shape parameters:

1 – case; *2* – basic supports; *3* – base; *4* – roller; *5*, *14*, *15*, *17* – angular displacement sensors; *6* – rocking chair; *7*, *18*, *23* – guides; *8* – rod, *9* – linear displacement sensor; *10*, *21* – compression spring; *11* – measuring support, *12* – base of the measuring support; *13* – roller; *16* – rod; *19* – frame; *20* – linear displacement sensor; *22*, *24* – transverse movement mechanism; *25*, *32* – electric drive; *26* – block for collecting, processing and storing information; *27* – full turn sensor; *28* – detail; *29* – part surface; *30* – mount; *31* – longitudinal movement device; *32* – power drive displacements [24]

model is provided with the possibility of its free rotation. This experimental assembly allows simulating the actual process of technological rotation of the support of the technological drum installed on two support rollers with the possibility of determining the accuracy parameters of the rolling surface shape with the experimental model of the measuring device. Control of adjustment and adjustment accuracy is carried out on a reference surface with a known radius of curvature, as well as end gauges.

Summarizing the above and based on accepted principles and approaches, the proposed technology includes the following sequence of actions:

1. Planned measurement of the riding ring rolling surface in order to detect the excess of permissible values of the shape accuracy parameters:
- 3D digital reconstruction of the surface;
- calculation of surface shape accuracy parameters;
- data recording and storing, determining the need for machining;

2. Simulation the process of shaping the machined surface for multi-pass machining:
- processing of measurement data and parameters of the processing module;

Fig. 14. Experimental sample of the measuring device with the control unit

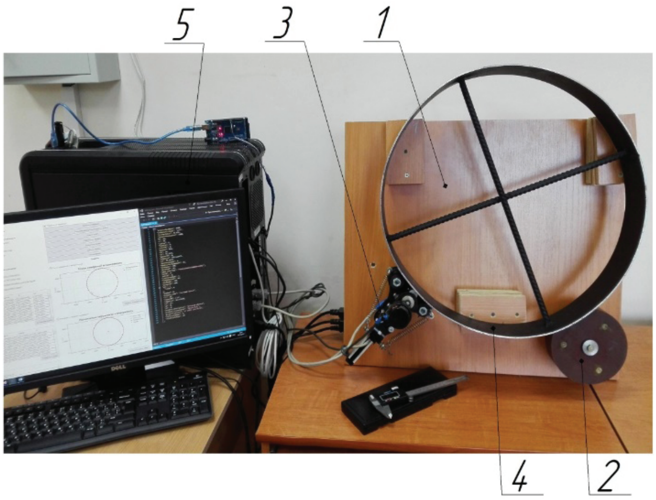

Fig. 15. Measurement on a laboratory sample:
1 – base plate; *2* – support roller; *3* – measuring device; *4* – rotation body model; *5* – computer

• calculation, construction and selection of the optimal machining route, as well as technological processing modes for each technological transition;

• data recording and storing;

3. Surface machining:

• multi-pass machining according to the calculated machining route;

• intermediate measurements control with determining the parameters of the surface shape accuracy or its part, if necessary;

• adjustment of the machining route based on control measurement data;

4. Final control measurement of surface shape accuracy parameters. Correction of the machining route, or completion of machining.

Conclusion

The presented method and virtual simulation of measurements for reduction processing make it possible to significantly reduce the processing time compared to the technology with active shape control and the traditional method, in which the allowance is removed with correction after each pass. The difference is that the machining route is calculated in advance and the measurement with correction is made only as needed.

It is determined that by providing a single technological base for each individual technological transition within the framework of the mobile technology of mechanical processing of the riding rings rolling surface of technological drums, the accuracy and speed of processing increase. In addition, inheritance of accuracy parameters for the entire surface is provided, which makes it possible to obtain a single profile of the longitudinal section of the entire surface. Thus, in the case of basing on a surface area with a minimum shape error, the number of technological working strokes necessary to achieve the required accuracy of the surface shape is reduced.

The processing of the entire remaining part of the surface, except for the area of basing, at each technological transition is significantly less efficient than the processing of only the surface area for rebasing until standard accuracy parameters are obtained at the processed area. Then basing is performed along the obtained surface area with the processing of the remaining surface. In this case (for the virtual model) the processing of 800 mm between areas took 15 working strokes, and in case of processing the entire surface at each transition it would take 52 working strokes.

Virtual modeling, control method and allowance determination method make it possible to obtain technical results and solve the problems of increasing the performance and ensuring the control accuracy of complex surfaces on coordinate measurement machines.

References

1. Phillips Kiln Services. Available at: http://www.pkse.co.uk (accessed 13.04.2022).

2. Boateng A.A. *Rotary kilns: transport phenomena and transport processes*. Elsevier, 2015. 390 p. ISBN 9780128038536.

3. Wei W., Peng Y., Du L., Cai Y. Design and mechanical behavior analysis of two-stall cement rotary kiln cylinder. *International Journal of Performability Engineering*, 2020, vol. 16, iss. 6, pp. 883–895. DOI: 10.23940/ijpe.20.06.p7.883895.

4. Lei X., Xiao Y., Chen G., Liu Y., Zhao X Anti-fatigue optimization of kiln shell at intermittent multi-body contact state. *Sichuan Daxue Xuebao (Gongcheng Kexue Ban) = Journal of Sichuan University. Engineering Science Edition*, 2014, vol. 46, iss. 6, pp. 185–190. (In Chinese).

5. Wei G., Tan Q. Measurement of shaft diameters by machine vision. *Applied Optics*, 2011, vol. 50, iss. 19, pp. 3246–3253. DOI: 10.1364/AO.50.003246.

6. Syusyuka E.N., Amineva E.Kh. Control of mobile equipment for the processing of marine shaft lines. *Journal of Physics: Conference Series*, 2021, vol. 2061, p. 012083. DOI: 10.1088/1742-6596/2061/1/012083.

7. Syusyuka E.N. Possibility of applying X-ray methods to control the surface quality of a shaft line after finishing. *Journal of Physics: Conference Series*, 2021, vol. 2061, p. 012022. DOI: 10.1088/1742-6596/2061/1/012022.

8. Zheng K., Zhang Y., Zhao C., Liu L. Rotary kiln cylinder deformation measurement and feature extraction based on EMD method. *Engineering Letters*, 2015, vol. 23, iss. 4, pp. 283–291.

9. Mogilny S., Sholomitskii A. Precision analysis of geometric parameters for rotating machines during cold alignment. *Procedia Engineering*, 2017, vol. 206, pp. 1709–1715. DOI: 10.1016/j.proeng.2017.10.702.

10. Li M., Yu J.P. Status and development of geometric measurement in industry. *Chinese Journal of Scientific Instrument*, 2017, vol. 38, iss. 12, pp. 2959–2971. (In Chinese).

11. Conte J., Santolaria J., Majarena A.C., Brau A., Aguilar J.J. Identification and kinematic calculation of laser tracker errors. *Procedia Engineering*, 2013, vol. 63, pp. 379–387. DOI: 10.1016/j.proeng.2013.08.190.

12. Farooqui S.A., Doiron T., Sahay C. Uncertainty analysis of cylindricity measurements using bootstrap method. *Measurement*, 2009, vol. 42, iss. 4, pp. 524–531. DOI: 10.1016/j.measurement.2008.09.008.

13. Koziołek S., Derlukiewicz D., Ptak M. Design process innovation of mechanical objects with the use of design for Six Sigma methodology. *Solid State Phenomena*, 2010, vol. 165, pp. 274–279. DOI: 10.4028/www.scientific.net/ssp.165.274.

14. Liu Y., Cheung C.F., Feng X., Wang C.J., Leach R.K. A self-calibration rotational stitching method for precision measurement of revolving surfaces. *Precision Engineering*, 2018, vol. 54, pp. 60–69. DOI: 10.1016/j.precisioneng.2018.05.002.

15. Ramaswami H., Kanagaraj S., Anand S. An inspection advisor for form error in cylindrical features. *International Journal of Advanced Manufacturing Technology*, 2009, vol. 40, pp. 128–143. DOI: 10.1007/s00170-007-1321-4.

16. Peng J., Chen D., Guo H., Zhong J., Yu Y. Variable optical null based on a yawing CGH for measuring steep acylindrical surface. *Optics Express*, 2018, vol. 26, iss. 16, pp. 20306–20318. DOI: 10.1364/OE.26.020306.

17. Zhao Z., Li B., Zhang G.,.Yu H, Shang M. Influence of eccentricity and tilt of cylindrical part's axis on the measurement results of its diameters. *Measurement*, 2019, vol. 138, pp. 232–239. DOI: 10.1016/j.measurement.2019.01.085.

18. Stamboliska Z., Rusinski E., Moczko P. *Proactive condition monitoring of low-speed machines*. Cham, Springer International Publishing, 2015, pp. 53–68. ISBN 978-3319104935, ISBN 3319104934.

19. Li X., Shen Y., Wang S. Dynamic modeling and analysis of the large-scale rotary machine with multi-supporting. *Shock and Vibration*, 2011, vol. 18, pp. 53–62. DOI: 10.1155/2011/541049.

20. Zheng K., Zhang Y., Liu L., Zhao C. An online straightness deviation measurement method of rotary kiln cylinder. *Tehnicki Vjesnik*, 2017, vol. 24 (5), pp. 1297–1305. DOI: 10.17559/TV-20150426160032.

21. Žiga A., Karač A., Vukojević D. Analytical and numerical stress analysis of the rotary kiln ring. *Tehnicki Vjesnik*, 2013, vol. 20, pp. 941–946.

22. Guo Y., Wang Y., Liu X. Real-time optical detection system for monitoring roller condition with automatic error compensation. *Optics and Lasers in Engineering*, 2014, vol. 53, pp. 69–78. DOI: 10.1016/j.optlaseng.2013.08.007.

23. Timofeev S.P., Khurtasenko A.V., Shrubchenko I.V., Voronkova M.N., Grinek A.V. *Izmeritel'noe ustroistvo dlya opredeleniya formy poverkhnostei krupnogabaritnykh detalei – tel vrashcheniya* [The measuring device for determining the surface shape of large size parts of rotation type]. Patent RF, no. 161400, 2016.

24. Grinek A.V., Timofeev S.P., Kondrat'ev S.I., Hurtasenko A.V. Sposob kontrolya parametrov geometricheskoi tochnosti sudovykh valoprovodov [Method of controlling geometric accuracy for ship shafts]. *Morskie intellektual'nye tekhnologi = Marine Intellectual Technologies*, 2020, no. 3, pt. 1, pp. 90–97. DOI: 10.37220/MIT.2020.49.3.011.

Conflicts of Interest

The authors declare no conflict of interest.